A Comprehensive Description of the Free Energy of an Intramolecular Hydrogen Bond as a Function of Solvation: NMR Study

Craig Beeson,† Nguyen Pham,† Gerald Shipps, Jr.,† and Thomas A. Dix*,†,‡

Contribution from the Departments of Chemistry and Biological Chemistry, The University of California, Irvine, California 92717

Received January 19, 1993

Abstract: Free energies of intramolecular hydroxyl (donor)-to-ether oxygen (acceptor) hydrogen bonds in hydroxyethers 10α-(hydroxymethyl)-2-oxabicyclo[4.4.0]decane (**1**) and 4-*tert*-butyl-2-(hydroxymethyl)-1-methoxycyclohexane (**2**) have been determined from changes in ^{1}H NMR vicinal coupling constants in a broad range of solvents (CCl_4 to D_2O). Various solvent polarity scales exhibited no direct correlation to changes in hydrogen bond ΔG values. Rather, a linear relationship between ΔG and the solvent's hydrogen bond basicity scale (β_{KT}) was demonstrated; slightly improved correlations could be achieved in certain cases by adding a solvent polarity term (either ϵ_K, or π^*) or a solvent hydrogen bond acidity term ($E_T(30)$) to the β_{KT} term. A van't Hoff analysis of the hydrogen bond thermodynamics of both **1** and **2** in $CDCl_3$ enabled determination of ΔH and ΔS values that were essentially intrinsic due to the limited assumptions attendant to the evaluation of intramolecular hydrogen bonds. The intrinsic ΔG values for both **1** and **2** ranged from −2.3 (CCl_4) to −0.5 kcal mol^{-1} (D_2O) to define the accessible range of strengths for a hydroxyl–ether hydrogen bond in liquid phase. The intrinsic ΔS values for **1** and **2** in $CDCl_3$, −3.5 ± 0.5 and −2.4 ± 0.5 cal mol^{-1} K^{-1}, respectively, are essentially equal despite a difference in the number of internal rotations compromised by hydrogen-bonding in each molecule. The lack of sensitivity to the number of internal rotations and the attenuated ΔS relative to that calculated in the gas phase indicated that losses in entropy attendant to changes in internal rotations may be of a smaller magnitude than previously thought in the liquid phase. The predominance of β_{KT} as a determinant of hydrogen bond free energies demonstrated that local dielectric has little effect on the strengths of hydrogen bonds. Thus, gas-phase ΔH values may be accessible in macromolecules depending upon the bonding geometry, the number of local acceptors, and the reorganizational energy expended to form the bond. These results have significance for the incorporation of solvation treatments into computer models, the prediction of biological structure and stability, and the design of small molecule and macromolecular architectures for molecular recognition.

Introduction

Hydrogen bonds, which are central structural elements in biomolecules, have been the subject of a wide variety of experimental[1] and theoretical[2] investigations. However, the development of a clear understanding of the various structural, electronic, and environmental factors that define observed hydrogen bond free energy (ΔG_{obs}) values, which would be invaluable to the interpretation of receptor–ligand and enzyme–substrate interactions, has been elusive. Recent attempts to probe these issues have dissected ΔG_{obs} values for the formation of enzyme–substrate[3] and receptor–ligand[4] complexes into intrinsic free energy (ΔG_i) values for specific electrostatic interactions involved in the complexes; the dissections have resulted in estimates of hydrogen bond ΔG_is ranging from −0.5 to −9.8 kcal mol^{-1}. In an alternative approach, thermochemical analyses of intramolecular interactions within engineered molecular architectures have avoided some of the assumptions attendant to the evaluation of the intermolecular complexes.[5] Collectively, these studies contribute to a data base from which conceptual foundations may be distilled, with the goal of developing general models for the energetics of electrostatic interactions. Incorporation of these empirical-based models into current theoretical models will ultimately lead to a refinement in the ability to predict the physicochemical properties of biological molecules.

The exquisite sensitivity of hydrogen bond energies to geometry, as inferred from surveys of X-ray and neutron crystal structure data bases,[6] has been well described with theoretical models;[2] however, experimental confirmation of the angular dependence of bond energies has only recently been available for gas-phase

* To whom correspondence should be addressed at the Department of Chemistry. Phone: (714) 856-5455. FAX: (714) 725-2210.

† Department of Chemistry.

‡ Department of Biological Chemistry.

(1) (a) Klotz, I. M.; Franzen, J. S. *J. Am. Chem. Soc.* **1962**, *84*, 3461. (b) Davis, J. C., Jr.; Deb, K. K. *Adv. Magn. Reson.* **1970**, *4*, 201. (c) Joesten, M. D.; Schaad, L. J. *Hydrogen Bonding*; Marcel Dekker: New York, 1974. (d) Scuster, P.; Zundel, G.; Sandorfy, C., Eds. *The Hydrogen Bond*; North Holland: Amsterdam, 1976. (e) Aaron, H. S. *Top. Stereochem.* **1980**, *11*, 1. (f) Meot-Ner (Mautner), M. *Acc. Chem. Res.* **1984**, *17*, 186. (g) Roseman, M. A. *J. Mol. Biol.* **1988**, *201*, 621. (h) Sneddon, S. F.; Tobias, D. J.; Brooks, C. L., III *J. Mol. Biol.* **1989**, *209*, 817. (i) Kossikoff, A. A.; Shpungin, J.; Sintchak, M. D. *Proc. Natl. Acad. Sci. U.S.A.* **1990**, *87*, 4468. (j) Gellman, S.; Dado, G. P.; Liang, G. B.; Adams, B. R. *J. Am. Chem. Soc.* **1991**, *113*, 1164.

(2) (a) Umeyama, H.; Morokuma, K. *J. Am. Chem. Soc.* **1977**, *99*, 1316. (b) Peters, D.; Peters, J. *J. Mol. Struct.* **1980**, *68*, 255. (c) Warshel, A. *Acc. Chem. Res.* **1981**, *14*, 284. (d) Hobza, P.; Mulder, F.; Sandorfy, C. *J. Am. Chem. Soc.* **1982**, *104*, 925. (e) Warshel, A.; Russell S. T. *Q. Rev. Biophys.* **1984**, *27*, 283. (f) Peters, D.; Peters, J. *Biopolymers* **1985**, *24*, 491. (g) Buckingham, A. D.; Fowler, P. W. *Can. J. Chem.* **1985**, *63*, 2018. (h) Hurst, G. J. B.; Fowler, P. W.; Stone, A. J.; Buckingham, A. D. *Int. J. Quantum Chem.* **1986**, *29*, 1223. (i) Cybulski, S. M.; Scheiner, S. *J. Phys. Chem.* **1989**, *93*, 6565. (j) Sharp, K. A.; Honig B. *Annu. Rev. Biophys. Biophys. Chem.* **1990**, *19*, 301. (k) Jorgensen, W. L. *J. Am. Chem. Soc.* **1989**, *111*, 3770. (l) Mitchell, J. B. O.; Price, S. L. *J. Comput. Chem.* **1990**, *11*, 1217. (m) Van Zandt, L. L.; Schroll, W. K. *J. Biomolec. Struct. Dyn.* **1990**, *8*, 431.

(3) Fersht, A. R.; Shi, J.; Knill-Jones, J.; Lowe, D. M.; Wilkinson, A. J., Blow, D. M.; Brick, P.; Carter, P.; Waye, M. M. Y.; Winter, G. *Nature* **1985**, *314*, 235. Bartlett, P. A.; Marlowe, C. K. *Science* **1987**, *235*, 569. Kati, W. M.; Wolfenden, R. *Biochemistry* **1989**, *28*, 1919.

(4) Williams, D. H.; Cox, J. P. L.; Doig, A. J.; Gardner, M.; Gerhard, U.; Kaye, P. T.; Allick, A. R.; Nicholls, I. A.; Salter, C. J.; Mitchell, R. C. *J. Am. Chem. Soc.* **1991**, *113*, 7020. Cox, J. P. L.; Nicholls, I. A.; Williams, D. H. *J. Chem. Soc., Chem. Commun.* **1991**, 1295. Williams, D. H. *Aldrichim. Acta* **1991**, *24*, 71. Williams, D. H. *Aldrichim. Acta* **1992**, *25*, 9.

(5) Beeson, C.; Dix, T. A. *Chem. Ind.* **1991**, 39. Beeson, C.; Dix, T. A. *J. Chem. Soc., Perkin Trans. 2* **1991**, 1913. Dix, T. A.; Beeson, C.; Bain, J. D.; Chamberlin, A. R. in *Proceedings of the 2nd Taniguichi Conference on Polymer Research—The Creation of Biofunctional Molecules*; Okamura, S., Tsuruta, T., Imanishi, Y., Sunamoto, J., Eds.; Kagaku-Dojin: Kyoto, 1991, p. 97. Beeson, C.; Dix, T. A. *J. Org. Chem.* **1992**, *57*, 4386.

0002-7863/93/1515-6803$04.00/0

dimers.[7] Experimental ΔG values for many hydrogen-bonded complexes in condensed phase (CCl_4), which have been correlated[8] with empirical hydrogen bond acidity and basicity scales, provide useful predictive schemes. However, a connection between the empirical scales[8] and theoretical models[2] has not yet been made. Similarly, empirical scales to account for the role of solvation as a determinant of conformational energies, binding constants, and reaction rates have been well developed[8-11] but typically lack a connection to the many semiempirical[12] and theoretical models[13] for solvation. Conversely, incorporation of a solvent physical property into solvation theories, such as solvent dielectric and reaction field theory,[14] often produces an incomplete description of electrostatic solvation.[8-13] With respect to hydrogen bonds, correlations of energies with solvent parameters have been made only over structurally limited ranges.[15] More inclusive solvent correlations clearly are required to fully describe the solvation of hydrogen-bonded molecules and the role of environment in promoting or attenuating hydrogen bond free energies.

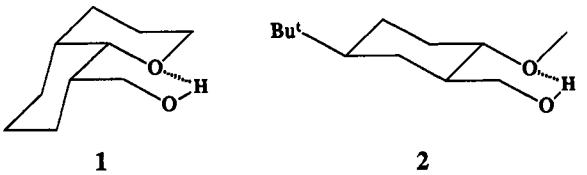

1 2

Figure 1. Structures of hydroxyethers **1** and **2** shown in their (approximate) hydrogen-bonded conformations.

This manuscript describes a combined ^1H NMR and IR[1e] analysis of hydroxyethers 10α-(hydroxymethyl)-2-oxabicyclo-[4.4.0]decane (**1**) and 4-*tert*-butyl-2-(hydroxymethyl)methoxycyclohexane (**2**) both of which form structurally equivalent intramolecular hydroxyl–ether hydrogen bonds (Figure 1).[16] These molecules are a part of an ongoing research program involving the design and implementation of conformation-based probes for biological electrostatic interactions.[5] The structural theme central to the design of **1** and **2** was the ability to form an intramolecular hydrogen bond between the hydroxymethyl donor and either a rotationally fixed, or free, ether acceptor (**1** and **2**, respectively). Further, it was intended that only a single, torsionally strained, hydroxymethyl rotamer in either molecule could form the bond; thus, a single, hydrogen-bond-stabilized rotamer is counterbalanced by two lower energy, nonbonded rotamers. The vicinal methine–hydroxymethylene ^1H–^1H NMR coupling constants (^3J values) were envisioned as probes of the hydroxymethyl rotameric populations, while IR was to be used to evaluate the degree of hydrogen-bonding. Evaluation of **2** in solvents ranging from CCl_4 to D_2O has enabled correlations to be made between the hydrogen bond ΔG_i and a number of solvent parameters, while evaluation of **1** and **2** in $CDCl_3$ at different temperatures enabled a van't Hoff analysis to describe the specific thermodynamic changes intrinsic to the hydrogen bond. These results have implications for the general description of hydrogen bonds in biological and biomimetic settings.

Results

Synthesis and Molecular Modeling. In the preparation of **1** (Scheme I), alkylation of the γ-carbon of ethyl 2-oxocyclohexanecarboxylate (**3**) with 3-chloroiodopropane with subsequent $NaBH_4$ reduction of the crude chloropropyl ketoester gave a mixture of hydroxyester diastereomers. The stereochemical outcome of the $NaBH_4$ reduction was not readily evident due to coincidental overlap of a number of downfield resonances and virtually identical R_f values (and boiling points) for the hydroxyester mixture; however, hydroxyester **4** (17% yield from **3**) was ultimately separable from the other two diastereomers by column

(6) Chen, C.; Parthasarathy, R. *Int. J. Pept. Protein Res.* **1978**, *11*, 9. (b) Vinogradov, S. N. In *Molecular Interactions*; Ratajczak, H., Orville-Thomas, W. J., Eds.; John Wiley & Sons: New York, 1980; Vol. 2, p 179. (c) Ceccarelli, C.; Jeffrey, G. A.; Taylor, R. *J. Mol. Struct.* **1981**, *70*, 255–271. (d) Baker, E. N.; Hubbard, R. E. *Prog. Biophys. Molec. Biol.* **1984**, *44*, 97. (e) Taylor, R.; Kennard, O. *Acc. Chem. Res.* **1984**, *17*, 320. (f) Etter, M. *Acc. Chem. Res.* **1990**, *23*, 120.

(7) Newton, M. D.; Jeffrey, G. A.; Takagi, S. *J. Am. Chem. Soc.* **1979**, *101*, 1997. Cheam, T. C.; Krimm, S. *J. Mol. Struct.* **1986**, *146*, 175. Mitchell, J. B. O.; Price, S. L. *Chem. Phys. Lett.* **1989**, *154*, 267. Kossiakoff, A. A.; Shpungin, J.; Sintchak, M. D. *Proc. Natl. Acad. Sci. U.S.A.* **1990**, *87*, 4468. Millen, D. J. *J. Mol. Struct.* **1990**, *237*, 1. Legon, A. C.; Millen, D. J. *Chem. Soc. Rev.* **1992**, *21*, 71.

(8) (a) Taft, R. W.; Gurka, D.; Joris, L.; Schleyer, P. v. R.; Rakshys, J. W. *J. Am. Chem. Soc.* **1969**, *91*, 4801. (b) Arnett, E. M.; Mitchell, E. J.; Murty, T. S. S. R. *J. Am. Chem. Soc.* **1974**, *96*, 3875. (c) Abraham, M. H.; Duce, P. P.; Morris, J. J.; Taylor, P. J. *J. Chem. Soc., Faraday Trans. 1* **1987**, *83*, 2867. (d) Abraham, M. H.; Greller, P. L.; Prior, D. V.; Taft, R. W.; Morris, J. J.; Taylor, P. J.; Laurence, C.; Berthelot, M.; Doherty, R. M.; Kamlet, M. J.; Abboud, J.-L. M.; Sraidi, K.; Guiheneuf, G. *J. Am. Chem. Soc.* **1988**, *110*, 8534.

(9) Reviews: (a) Malecki, J. In *Molecular Interactions*; Ratajczak, H., Orville-Thomas, W. J., Eds.; John Wiley & Sons: New York, 1982; Vol. 3, p 183. (b) Reichardt, C. *Molecular Interactions*; Ratajczak, H., Orville-Thomas, W. J., Eds.; John Wiley & Sons: New York, 1982; Vol. 3, p 241. (c) Kamlet, M. J.; Abboud, J. M.; Abraham, M. H.; Taft, R. W. *J. Org. Chem.* **1983**, *48*, 2877. (d) Taft, R. W.; Abboud, J.-L. M.; Kamlet, M. J.; Abraham, M. H. *J. Solution Chem.* **1985**, *14*, 153. (e) Abraham, M. H.; Grellier, P. L.; Abboud, J. M.; Doherty, R. M.; Taft, R. W. *Can. J. Chem.* **1988**, *66*, 2673. (f) Suppan, P. *J. Photochem. Photobiol.* **1990**, *50*, 293.

(10) Studies of conformational equilibria: (a) Abraham, R. J. *J. Phys. Chem.* **1969**, *73*, 1192. (b) Abraham, R. J.; Gatti, G. *J. Chem. Soc. (B)* **1969**, 961. (c) Oi, N.; Coetzee, J. F. *J. Am. Chem. Soc.* **1969**, *91*, 2478. (d) Abraham, R. J.; Griffiths, L. *Tetrahedron* **1981**, *37*, 575. (e) Chastrette, M.; Carretto J. *Tetrahedron* **1982**, *38*, 1615. (f) Abraham, M. H.; Xodo, L. E. *J. Chem. Soc., Perkin Trans. 2* **1982**, 1503. (g) Bekarek, V.; Jurina, J. *Collect. Czech. Chem. Commun.* **1982**, *47*, 1060. (h) Chen, J. S.; Shirts, R. B.; Lin, W. C. *J. Phys. Chem.* **1986**, *90*, 4970. (i) Latypov, Sh. K.; Klochkov, V. V. *Izv. Akad. Nauk SSSR, Ser. Khim.* **1990**, *1*, 41. (j) Gorbachuk, V. V.; Smirnov, S. A., Solomonov, B. N.; Konovalov, A. I. *Zhur. Obshchei Khim.* **1990**, 60, 1200. (k) Klochkov, V. V.; Latypov, A. V.; Il'yasov, A. V.; Aganov, A. V. *Izv. Akad. Nauk SSSR, Ser. Khim.* **1990**, *6*, 1300. (l) Smithrud, D. B.; Diederich, F. *J. Am. Chem. Soc.* **1990**, *112*, 339. (m) Abraham, M. H.; Abraham, R. J.; Leonard, P.; True, N. S.; Suarez, C. *J. Chem. Soc., Perkin Trans. 2* **1991**, 463. (n) Ferguson, S. B.; Sanford, E. M.; Seward, E. M.; Diederich, F. *J. Am. Chem. Soc.* **1991**, *113*, 5410. (o) Smithrud, D. B.; Wyman, T. B.; Diederich, F. *J. Am. Chem. Soc.* **1991**, *113*, 5420. (p) Kolling, O. W. *J. Phys. Chem.* **1992**, *96*, 1729. (q) Drago, R. S. *J. Chem. Soc., Perkin Trans. 2* **1992**, 1827. (r) Gajewski, J. J. *J. Org. Chem.* **1992**, *57*, 5500.

(11) Solvent hydrogen bond acidity and basicity: (a) Fawcett, W. R.; Krygowski, T. M. *J. Am. Chem. Soc.* **1975**, *97*, 2143. (b) Fawcett, W. R.; Krygowski, T. M. *Aust. J. Chem.* **1975**, *28*, 2115. (c) Krygowski, T. M.; Radomski, J. P.; Rzeszowiak, A.; Wrona, P. K.; Reichardt, C. *Tetrahedron* **1981**, *37*, 119. (d) Swain, C. G.; Swain, M. S.; Powell, A. L.; Alunni, S. *J. Am. Chem. Soc.* **1983**, *105*, 502. (e) Catalan, J.; Couto, A.; Gomez, J.; Saiz, J. L.; Laynez, J. *J. Chem. Soc., Perkin Trans. 2* **1992**, 1181.

(12) For general reviews of computational methods, see: *The Chemical Physics of Solvation*; Dogonadze, R. R., Kalman, E., Kornyshev, A. A., Ulstrup, J., Eds.; Elsevier: Amsterdam, 1985; Vol. 1. Richards, W. G.; King, P. M.; Reynolds, C. A. *Protein Eng.* **1989**, *2*, 319. Recent semiempirical methods: Still, W. C.; Tempczyk, A.; Hawley, R. C.; Hendrickson, T. *J. Am. Chem. Soc.* **1990**, *112*, 6127. Jean-Charles, A.; Nicholls, A.; Sharp, K.; Honig, B.; Tempczyk, A.; Hendrickson, T. F.; Still, W. C. *J. Am. Chem. Soc.* **1991**, *113* 1454. Cramer, C. J.; Truhlar, D. G. *Science* **1992**, *256*, 213.

(13) Dosen-Micovic, L.; Allinger, N. L. *Tetrahedron* **1978**, *34*, 3385. Warshel, A. *J. Phys. Chem.* **1979**, *83*, 1640. Jorgensen, W. L. *J. Phys. Chem.* **1983**, *87*, 5304. Warshel, A.; Russell, S. T.; Churg, A. K. *Proc. Natl. Acad. Sci. U.S.A.* **1984**, *81*, 4785. Shanmugasundaram, V.; Thiyagarajan, P. *J. Indian Chem. Soc.* **1986**, *63*, 589. Schaefer, T.; Sebastian, R.; Li, H. Y.; Quach, T. *Can. J. Chem.* **1990**, *68*, 996. Wong, M. W.; Frisch, M. J.; Wiberg, K. B. *J. Am. Chem. Soc.* **1991**, *113*, 4776. Luzhkov, V.; Warshel, A. *J. Am. Chem. Soc.* **1991**, *113*, 4491. Sharp, K.; Jean-Charles, A.; Honig, B. *J. Phys. Chem.* **1992**, *96*, 3822. Tvaroska, I.; Bleha, T. *Collect. Czech. Chem. Commun.* **1980**, *45*, 1883. Pettitt, B. M.; Karplus, M.; Rossky, P. J. *J. Phys. Chem* **1986**, *90*, 6335. Meyer, A. Y. *J. Mol. Struct.* **1989**, *195*, 147.

(14) Onsager, L. *J. Am. Chem. Soc.* **1936**, *58*, 1486. Kirkwood, J. G.; Westheimer, F. H. *J. Chem. Phys.* **1938**, *6*, 506.

(15) (a) Allerhand, A.; Schleyer, P. v. R. *J. Am. Chem. Soc.* **1963**, *85*, 371. (b) Christian, S. D.; Johnson, J. R.; Affsprung, H. E.; Kilpatrick, P. J. *J. Phys. Chem.* **1966**, *70*, 3376. (c) Sherry, A. D.; Purcell, K. F. *J. Am. Chem. Soc.* **1972**, *94*, 1853. (d) Guidry, R. M.; Drago, R. S. *J. Phys. Chem.* **1974**, *78*, 454. (e) Biali, S.; Rappoport, Z. *J. Am. Chem. Soc.* **1984**, *106*, 5641. (f) Nadler, E. B.; Rappoport, Z. *J. Am. Chem. Soc.* **1989**, *111*, 213. (g) Schneider, H.-J.; Juneja, R. K.; Simova, S. *Chem. Ber.* **1989**, *122*, 1211. (h) Catalan, J.; Gomez, J.; Couto, A.; Laymez, J. *J. Am. Chem. Soc.* **1990**, *112*, 1678.

(16) For related studies of intramolecular hydroxyl–ether and hydroxyl–hydroxyl hydrogen bonds, see: (a) Kuhn, L. P.; Wires, R. A. *J. Chem. Soc.* **1964**, 2161. (b) Bodot, H.; Fediere, J.; Pouzard, G.; Pujol, L. *Bull. Soc. Chim. Fr.* **1968**, 3260. (c) Kingsbury, C. A. *J. Org. Chem.* **1970**, *35*, 1319. (d) Auerbach, R. A.; Kingsbury, C. A. *Tetrahedron* **1971**, *27*, 2069. (e) Landmann, B.; Hoffman, R. W. *Chem. Ber.* **1987**, *120*, 331. (f) Khot, M. S.; Smith, D. A.; McMillan, G. R.; Sukenik, C. N. *J. Org. Chem.* **1992**, *57*, 3799.

Scheme I Synthetic Scheme for the Preparation of Hydroxyethers **1** and **2** and Diethers **9** and **10**[a]

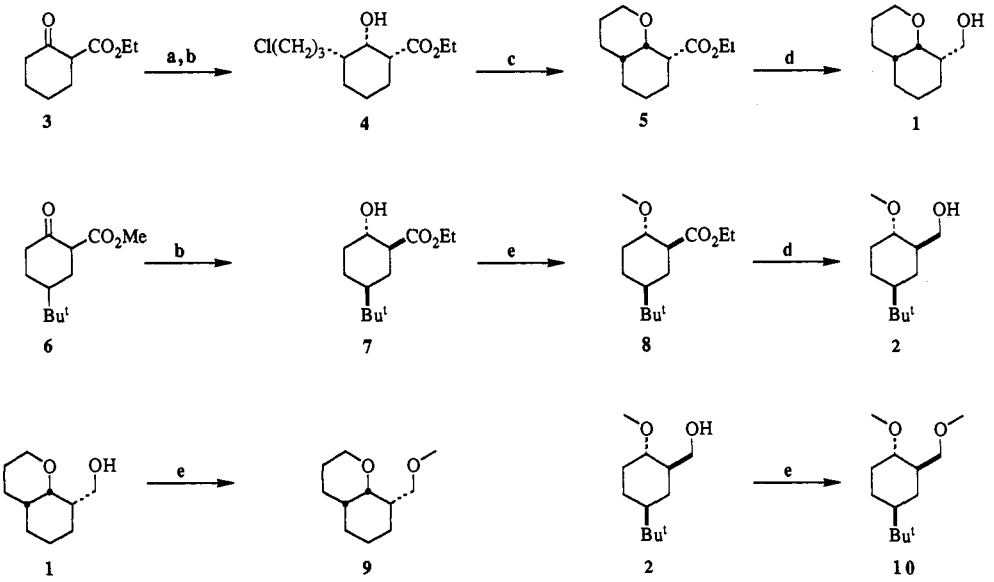

[a]LDA (2 equiv), $I(CH_2)_3Cl$; (b) $NaBH_4$; (c) NaH; (d) $LiAlH_4$; (e) NaH, CH_3I.

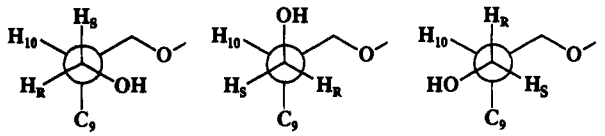

g⁻ g⁺ t

Hydroxyether 1

Conformer	CH--CH_2	CH_2--OH	$\Delta E_{(g)}$ kcal mol⁻¹
1	g⁻	g⁺	0
2	g⁺	g-	1.2
3	g⁺	t	1.3
4	t	t	1.5
5	g⁺	g⁺	2.3
6	g⁻	t	4.0

Methoxyether 9

Conformer	CH-CH_2	CH_2-OCH_3	$\Delta E_{(g)}$ kcal mol⁻¹
1	g⁺	t	0
2	t	t	0.2
3	g⁺	g⁺	2.0
4	t	g⁻	2.2
5	g⁻	t	2.4

Figure 2. Illustration of the three hydroxymethyl C–C rotamers for hydroxyether **1** and diether **9** and the molecular mechanics[18a] calculated relative energies.

chromatography. Evidence for all-*cis* stereochemistry in **4** existed: the narrow resonance for the proton H(2) observed in the ^1H NMR spectrum reflected its equatorial disposition, as the other two possible diastereomers would have an axial H(2) with at least one axial–axial ^1H–^1H vicinal coupling constant. The relative stereochemistry was confirmed by cyclization of **4** (*via* NaH) to ether **5**, whose relative stereochemistry was readily assigned *via* spin coupling and NOEs in a well-dispersed ^1H NMR spectrum. Subsequent reduction of the carboxylate of **5** ($LiAlH_4$) afforded the hydroxyether **1** in a 42% yield from **4**. In the preparation of **2** (Figure 2), the $NaBH_4$ reduction of β-ketoester **6** gave hydroxyester **7** as the major diastereomer (65%); factors controlling the stereochemistry of this reduction have been discussed previously.[17] Alkylation of hydroxyester **7** to give the ether **8** and subsequent reduction of the carboxylate afforded hydroxyether **2** in a 55% yield from **7**. Methylation of **1** and **2** (Figure 2) provided diethers **9** and **10**, respectively, which were used to evaluate the role of solvation as a determinant of hydroxymethyl C–C rotameric populations in the absence of an intramolecular hydrogen bond.

The chair–chair conformational transitions of the oxadecalin and cyclohexane rings for **1** and **2**, respectively, are severely biased (>4 kcal/mol, as estimated with molecular mechanics calculations[18a]) toward the illustrated conformers (Figure 1); thus, the only significant conformational transitions anticipated were rotations about the hydroxymethyl C–C and C–O bonds (and the methoxy C–OCH_3 bond in **2**). Relative energies ($\Delta E_{(g)}$) of the hydroxyether and diether conformations, as estimated with molecular mechanics calculations[18] (gas phase with a distance-dependent dielectric of 1), are provided in Figures 2 and 3. For both **1** and **2**, the hydrogen-bonded conformations (conformers 1 in Figures 2 and 3, respectively) were identified as torsionally strained but lowest in total energy; no other conformations were identified in which a significant intramolecular hydrogen bond existed. Predicted hydrogen bond geometries for **1** and **2**, as calculated with molecular mechanics (MM2), semiempirical (AM1), and *ab initio* (RHF/3-21G*) methods,[18] are listed in Table I. To calibrate the calculated geometries, the intramolecular hydroxymethyl–anomeric oxygen hydrogen bond in D-α-fructopyranose, observed in neutron diffraction studies,[19] was also evaluated; experimental and predicted geometries are listed in Table II.

IR Analyses. IR spectroscopy, in which the time scale allows for direct observation of the free and hydrogen-bonded hydroxyl stretch resonances (ν_{OH}), is a common method for determining the extent of intramolecular hydrogen-bonding.[1e] Usually, a structural analog of the hydrogen-bonding molecule lacking the hydrogen bond acceptor is used to calculate the extinction coefficient for the free ν_{OH}, which is subsequently used to calculate the amount of free ν_{OH} for the hydrogen-bonded species. The concentration of bonded ν_{OH} must subsequently be determined from the difference between free ν_{OH} and total concentrations, as estimation of the extinction coefficient for the bonded ν_{OH}

(17) Beeson, C.; Pham, N.; Dix, T. A. *Tetrahedron Lett.* **1992**, *33*, 2925.
(18) (a) Macromodel V3: Mohamidi, F.; Richards, N. G. J.; Guida, W. C.; Liskamp, M.; Lipton, M.; Caufield, C.; Chang, G.; Hendrickson, T.; Still, W. C. *J. Comput. Chem.* **1990**, *11*, 440. (b) Spartan, Wavefunction V1.0(5), Inc., Irvine, CA.
(19) Takagi, S., Jeffrey, G. A. *Acta Crystallogr.* **1977**, *B33*, 3510.

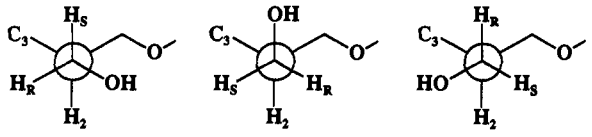

Hydroxyether 2

Conformer	CH--CH_2	CH_2--OH	CH--OCH_3	$\Delta E_{(g)}$ kcal mol^{-1}
1	g⁻	g⁺	t	0
2	g⁺	t	t	1.5
3	t	t	t	1.6
4	g⁻	g⁺	t	2.1
5	g⁻	g⁻	g⁺	2.0
6	g⁺	g⁺	t	2.5

Dimethoxyether 10

Conformer	CH--CH_2	CH_2--OCH_3	CH--OCH_3	$\Delta E_{(g)}$ kcal mol^{-1}
1	g⁺	t	t	0
2	t	t	t	0.2
3	t	g⁺	t	1.8
4	t	t	g⁺	2.0
5	g⁺	t	g⁺	2.3
6	g⁻	t	t	2.4

Figure 3. Illustration of the three hydroxymethyl C–C rotamers for hydroxyether **2** and diether **10** and molecular mechanics[18a] calculated relative energies.

Table I. Calculated Hydrogen Bond Geometries for Hydroxyethers **1** and **2**[a]

	1			**2**		
	MM2	AM1	3-21G*	MM2	AM1	3-21G*
$H_d\cdots O_a$	2.05 Å	2.14 Å	1.86 Å	2.09 Å	2.15 Å	1.85 Å
O—O	2.79 Å	2.87 Å	2.68 Å	2.80 Å	2.89 Å	2.68 Å
∠O—$H_d\cdots O_a$	134°	131°	140°	131°	132°	142°

[a] In the first column, the subscript d refers to the hydrogen bond donor and the subscript a to the hydrogen bond acceptor.

Table II. Calculated and Experimental[19] Hydrogen Bond Geometry for the Hydroxymethyl–Anomeric Oxygen Intramolecular Hydrogen Bond of D-α-Fructopyranose[a]

	experimental	MM2	AM1	3-21G*
$H_d\cdots O_a$	2.35 Å	2.25 Å	2.58 Å	2.33 Å
O···O	2.75 Å	2.71 Å	2.92 Å	2.73 Å
∠O—$H_d\cdots O_a$	104°	109°	101°	104°

[a] In the first column, the subscript d refers to the hydrogen bond donor and the subscript a to the hydrogen bond acceptor.

from a structural analog is hampered by an exquisite sensitivity of an intramolecular ν_{OH} to local geometry.[1e,16a] 2-Methylpropanol, a mimic of the hydrocarbon portion of the ring proximal to the hydroxymethyl substituent of **1** and **2**, was chosen as a structural analog to estimate the extinction coefficient for the free ν_{OH}. Integration of ν_{OH} at 3620 cm^{-1} for 2-methylpropanol in $CHCl_3$ (1 mM to 10 mM) gave a linear relation with an extinction coefficient of 0.236 ± 0.004 mM^{-1} cm^{-1}; no bonded ν_{OH} stretch, which would have indicated the presence of intermolecular hydrogen-bonding, was observed in this concentration range. Analysis of **1** in $CHCl_3$ produced IR spectra (Figure 4) in which both free ν_{OH} (3608 cm^{-1}) and bonded ν_{OH} (3479 cm^{-1}) were observed; the invariance in the integrated ratio between 1 and 20 mM **1** indicated that the bonding was exclusively intramolecular.

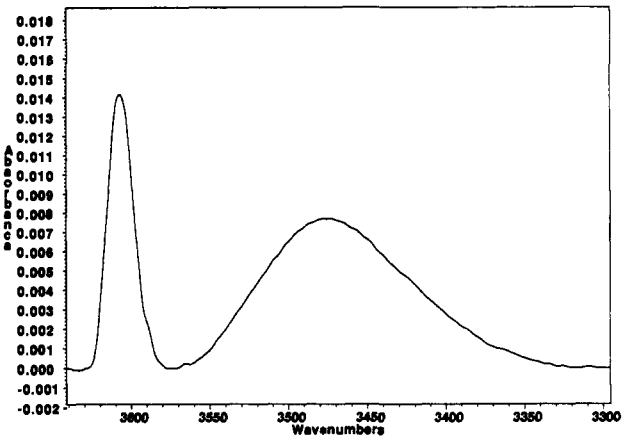

Figure 4. Illustrative IR spectrum for hydroxyether **1** in $CHCl_3$. The spectrum has been base line corrected for aesthetics, while integrations were done on uncorrected spectra. The narrow and broad resonances at 3618 and 3479 cm^{-1}, respectively, were assigned to the free and bonded conformations, respectively.

From the extinction coefficient for 2-methylpropanol, the mole fraction of the hydrogen-bonded state (χ^{HB}) for **1** was estimated to be 0.63 ± 0.02 at 20 °C.

The IR spectra of **2** were similar to those of **1**, with free and bonded ν_{OH} at 3610 cm^{-1} and 3481 cm^{-1}, respectively. However, the use of 2-methylpropanol as a model for the free ν_{OH} of **1** consistently gave χ^{HB} <0.05, which was clearly inconsistent with the ^{1}H NMR data (see below). The failure of 2-methylpropanol as a model for the nonbonded state of **2** presumably reflects coupling between the methoxy and ν_{OH} dipoles which would dramatically affect the resonance intensity[20] and represents an inherent compromise in the use of structurally modified compounds to model the free ν_{OH}. The reasonable agreement between the IR and NMR data for **1** (see below) offers support for the use of 2-methylpropanol as a model for the nonbonded rotamers of **1** and, thus, would argue that the relative orientations of the ether dipole and ν_{OH} dipole in the nonbonded states of **2** differ from those in **1**. Indeed, the calculated geometries of the lowest energy nonbonded rotamers of **1** and **2** differ with respect to the relative orientations of the hydroxyl and methoxy dipoles. Due to the nearly identical predicted hydrogen bond geometries of **1** and **2** and consequently nearly identical relative dipolar orientations, an extinction coefficient for the bonded ν_{OH} of **1** was calculated and used to estimate the degree of hydrogen-bonding in **2**, giving χ^{HB} = 0.74 ± 0.03 at 20 °C.

^{1}H NMR and van't Hoff Analyses. In the absence of coupling with the hydroxyl proton,[21] the hydroxymethylene H(10′) protons of **1** produced the AM portion of an AMX spin system in the ^{1}H NMR spectra in $CDCl_3$ (Figure 5a); simulation[22] of the observed spectra confirmed that the signals were first order, and thus measured peak separations were true ^3J values. In spectra for which the hydroxyl exchange rate was intermediate, the upfield H(10′) resonance was extremely broadened while the downfield H(10′) resonance was virtually unaffected. Decoupling of the *HO* resonance in slow exchange spectra demonstrated a coupling constant (9.30 Hz) with the upfield resonance that was larger than that with the downfield resonance (1.44 Hz). In the hydrogen-bonded conformer of **1** (Figure 2), the *pro-R* H(10′) is approximately *trans* to the hydroxyl proton and would be expected to be more strongly coupled to the hydroxyl proton than

(20) *Spectrometric Identification of Organic Compounds*, 5th ed.; Silverstein, R. M., Bassler, G. C., Morrill, T. C., Eds; Wiley & Sons: New York, 1991; pp 91–95.

(21) Coupling with the hydroxyl proton was removed with the addition of trace CF_3CO_2H to solutions in which the exchange rate was initially intermediate or with decoupling for slow exchange spectra. Spectra were independent of concentration (0.5–20 mM).

(22) Chemical shift differences in simulated (GE software) and observed spectra differed by <0.02 Hz.

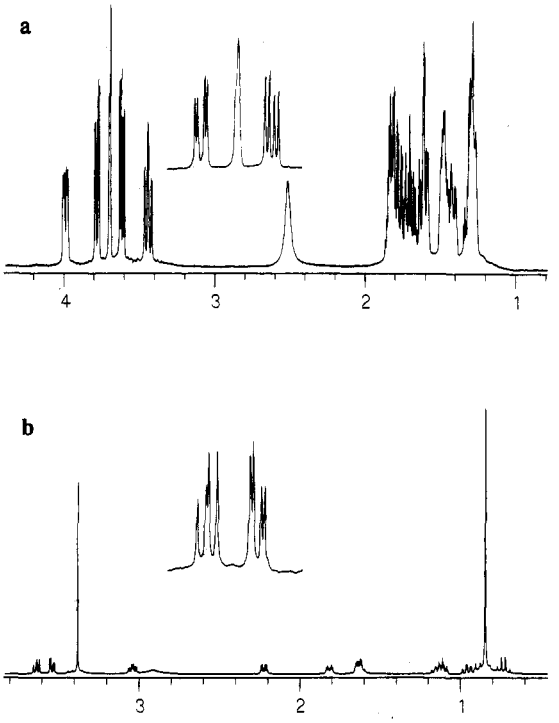

Figure 5. ^{1}H NMR spectra of (a) hydroxyether **1** and (b) hydroxyether **2** in $CDCl_3$ at 20 °C in which the hydroxyl *HO* resonances are exchange decoupled. The AM portions of the hydroxymethylene AMX spin system are expanded and offset for illustration.

would be the *pro-S* hydrogen;[23] thus, the upfield and downfield H(10)′ resonances were assigned as *pro-R* and *pro-S*, respectively. A decrease in temperature decreased the H(10)-H(10′) ^3J values for **1** in $CDCl_3$ (Figure 1a, supplementary material) due to increased hydrogen-bonding at lower temperatures which favors conformer 1 (Figure 2), in which both ^3J values are small.[24] However, the change in ^3J values for **1**, which reflected changes in the population of conformer 1, were not immediately amenable to a van't Hoff analysis due to the lack of rigorous intrinsic ^3J values for each of the hydroxymethyl C–C rotamers.[25]

The IR analysis of **1** at 20 °C provided a link between observed hydroxymethyl ^3J values and the degree of hydrogen-bonding: a two-state model was assumed in which the hydroxyether alternated between a single hydrogen-bonded conformer distinguished by a single set of intrinsic *pro-R* and *pro-S* ^3J values (^3J_i) and a second state consisting of nonbonded conformations distinguished by a set of average *pro-R* and *pro-S* intrinsic ^3J values ($\langle^3J_i\rangle$). Thus, the observed ^3J for either proton ($^3J_{obs}$) could be expressed as a weighted average:

$$^3J_{obs} = \chi^{HB}(^3J_i) + (1 - \chi^{HB})\langle^3J_i\rangle \qquad (1)$$

Inclusion of the IR-calculated mole fraction of hydrogen-bonded hydroxyl (χ^{HB}) in $CHCl_3$ at 20 °C into eq 1 provided a restraint to iteratively estimate values for ^3J_i and $\langle^3J_i\rangle$ that gave the most consistent χ^{HB} for $^3J_{obs}$ at each temperature. The three assumptions and attendant justifications inherent to this model are as follows. (1) The intrinsic ^3J values are not temperature dependent. The ^3J values of protons not involved in the hydroxymethyl rotation were invariant during temperature changes. (2) The relative populations with different C–C rotameric dispositions within the ensemble of nonbonded conformations (and, thus, $\langle^3J_i\rangle$ values)

(23) Fraser R. P.; Kaufman, M.; Morand, P. *Can. J. Chem.* **1969**, 47, 403. Watanabe, S. J. *J. Mol. Struct.* **1980**, *64*, 285.
(24) Haasnoot, C. A. G.; DeLeeuw, F. A. A. M.; Altona, C. *Tetrahedron* **1980**, *36*, 2783
(25) Although ^3J values predicted from a Karplus relation could be used to calculate the rotamer populations (for example see, ref 16f), it was decided that the data were amenable to a direct calculation of the intrinsic ^3J values (see also ref 27).

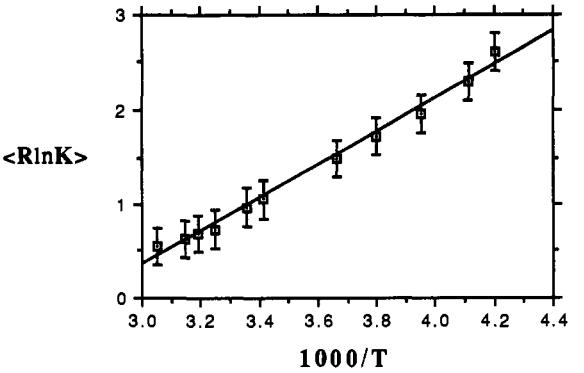

Figure 6. Van't Hoff graph for hydroxyether **1** in $CDCl_3$; $\langle R \ln K\rangle$ = R ln K_{eq} for hydrogen-bonded conformation (kcal mol^{-1}) averaged from the *pro-R* and *pro-S* hydroxymethylene resonances. Error bars are the standard errors.

are not temperature dependent. In ^{1}H NMR spectra of the diether **9** in $CDCl_3$, the H(10′) ^3J values (6.44 and 7.29 Hz) were invariant (±0.02 Hz) during temperature changes. The diether **9**, on the basis of the molecular mechanics calculations (Figure 2), primarily populated conformations with C–C rotameric dispositions of g^+ and t that were similar to the ensemble of nonbonded conformations for **1**. (3) χ^{HB} is equal to the mole fraction of all conformations with a C–C rotameric disposition of g^-. In the molecular mechanics calculations for **1**, the lowest energy *nonbonded* conformation in which the hydroxymethyl C–C rotamer is g^- (conformer 6, Figure 2) was 2.8 kcal mol^{-1} higher in energy than the lowest energy nonbonded conformation.

The computer-predicted ^3J values[18,24] (*pro-R*, *pro-S* = 2.8, 1.3 Hz) for the hydrogen-bonded conformer of **1** (Figure 2) were used as initial inputs for ^3J_i in eq 1; the ^3J_i inputs were subsequently varied to obtain the most consistent set of χ^{HB} for $^3J_{obs}$ values at each temperature; the best fit was obtained with *pro-R* ^3J_i and $\langle^3J_i\rangle$ values of 3.15 and 7.27 Hz, respectively, and *pro-S* ^3J_i and $\langle^3J_i\rangle$ values of 1.15 and 6.16 Hz, respectively. Internal consistency between the IR and ^{1}H NMR analyses was evident from the similarity of calculated ^3J_i values with those predicted from the Karplus relation.[18,24] The χ^{HB} values calculated at each temperature were converted to K_{eq}s for the conformational transition from nonbonded (an ensemble) to bonded states; a van't Hoff analysis (Figure 6) gave $\Delta H = -1.8 \pm 0.2$ kcal mol^{-1} and $\Delta S = -4.9 \pm 0.5$ cal mol^{-1} K^{-1} (error limits determined from the linear regression variance and reproducibility of J values (±0.15 Hz). The slight curvature apparent in the data was not taken as evidence for a ΔC_p change or the presence of systematic errors in measuring small coupling constants—graphs of van't Hoff data for the individual *pro-R* and *pro-S* ^3J values (Figures 1b,c, supplementary material) demonstrated only slight curvature for the *pro-R* hydrogen (and no curvature for the *pro-S* hydrogen data, which are dependent on measuring a smaller ^3J value) and thus may represent a small dependence of the *pro-R* ^3J on a temperature-dependent variable (*i.e.*, dielectric, see below).

The ^{1}H NMR analysis of hydroxyether **2** was similar to that for **1**; however, the hydroxymethyl H(2′) resonances for **2** produced the AM portion of an AMX spin system (in the absence of hydroxyl coupling) that was partly tinged with second-order effects (Figure 5b). Thus, spectral simulations[22] were required to correct the observed frequency differences to enable generation of ^3J values; typical corrections were <0.20 Hz. As with **1**, decouplings of the *HO* resonance in slow exchange spectra were used to assign the upfield and downfield H(2′) resonances as *pro-R* and *pro-S*, respectively; however, the resonances were also assigned from the magnitude of the H(2)–H(2′) ^3J values. In the hydrogen-bonded conformation of **2** (conformer 1, Figure 3), the *pro-R* and *pro-S* H(2′) resonances would have a small and large H(2)–H(2′) ^3J value, respectively. In nonbonded conformations in which the hydroxymethyl C–C rotamer is t, the relative magnitudes of

H(2′) ^3J values would be reversed relative to those in the bonded conformation, while those nonbonded conformations with a C–C g^+ rotamer would have small ^3J values. Thus, the observed *pro-R* and *pro-S* ^3J values for **2** in $CDCl_3$ at 20 °C, 3.06 and 8.40 Hz, respectively, were readily assigned and demonstrated that the hydrogen-bonded conformer was significantly populated. (While the observed ^3J values are consistent with significant population of either the g^- (bonded) or t conformation, the presence of a significant bonded ν_{OH} stretch in the IR spectra confirms that it is the g^- conformation that is being populated.) Conversely, molecular mechanics calculations for the diether **10** predicted a predominant population of conformations with only g^+ and t methoxymethyl C–C rotamers; the corresponding H(2′) ^3J values for **10** in $CDCl_3$ were 6.47 and 2.87 Hz, listed upfield to downfield, respectively. Unlike the diether **9**, the upfield and downfield H(2′) resonances reasonably could be assigned as *pro-R* and *pro-S*, respectively, in consideration of their relative magnitudes.

The method used to estimate intrinsic ^3J values for hydroxyether **1** was also used for **2** with one notable exception—the methoxymethyl H(2′) ^3J values for the diether **10**, unlike those for the diether **9**, were temperature dependent. The two classes of nonbonded conformations of **2**, distinguished by the hydroxymethyl C–C dihedral of g^+ and t, differ substantially in molecular dipoles[26] and would thus be expected to respond to the temperature-dependent change in dielectric.[10] The diether **10** was predicted (Figure 3) to populate only conformations with methoxymethyl C–C dihedrals of g^+ and t in which the calculated dipole moments[26] and relative steric energies (Figure 3) were similar to those for **2**; thus, observed temperature-dependent changes in ^3J for **10** were used to approximate intrinsic changes in ^3J for the nonbonded conformations of **2**. Thus, the IR-determined χ^{HB} for **2** in $CHCl_3$ at 20 °C and the observed ^3J values for **2** in $CDCl_3$ at 20 °C were used as restraints in eq 1 to iteratively solve for intrinsic ^3J_i and $\langle ^3J_i \rangle$ values that gave the most consistent χ^{HB} for observed ^3J values at each temperature. The observed changes in the *pro-R* and *pro-S* H(2′) ^3J values for the diether **10**, -3.3×10^{-3} and 1.2×10^{-3} Hz K^{-1}, respectively, were applied to the $\langle ^3J_i \rangle$ values prior to the calculation of χ^{HB} at each temperature. The J_i and $\langle J_i \rangle$ values estimated for the *pro-R* H(2′) at 20 °C were 2.30 and 5.83 Hz, respectively, while those estimated for the *pro-S* H(2′) were 10.30 and 2.93 Hz, respectively.[27] A van't Hoff analysis of the corresponding K_{eq}s gave $\Delta H = -1.7 \pm 0.1$ kcal mol^{-1} and $\Delta S = -3.8 \pm 0.4$ cal mol^{-1} K^{-1}. As with the van't Hoff analysis of **1**, it was assumed that the change in ΔC_p was negligible over the temperature range examined.

Intrinsic Thermodynamics. Determination of the thermodynamics for the intramolecular hydrogen bond of **1** and **2** offered a facile method for estimating the intrinsic thermodynamics, as many of the assumptions attendant to the evaluation of intermolecular hydrogen-bonded adducts are absent. The ΔS_{obs} values were increased by R ln 2 to account for averaging of two hydroxymethyl C–C rotamers for $\langle ^3J_i \rangle$, giving intrinsic ΔS_i values of -3.5 ± 0.3 and -2.4 ± 0.4 cal mol^{-1} K^{-1} for hydroxyethers **1** and **2**, respectively. Corrections to ΔH_{obs} for the steric strain inherent to the hydrogen-bonded conformations required an evaluation of the population of the bonded conformation in which the hydrogen bond interaction was removed. The steric strain was determined from the conformational energies calculated from the MM2 force field,[18a] which does not include an explicit hydrogen bond parameter. Subtraction of the MM2 electrostatic energy from the total energy gave "steric energies", composed of bond stretch, bond angle, torsion, and van der Waals terms, of 1.2 and 1.5 kcal mol^{-1} (average 1.4 kcal mol^{-1}) for **1** and **2**, respectively. If the molecular mechanics strain energies were reasonable, the population of g^- rotor might approach 10% in the absence of a hydrogen bond. Such a population would have produced an approximately 1-Hz perturbation in the expected J values for solvents in which the intramolecular hydrogen-bonding was not observed—thus, is is assumed that the molecular mechanics strain values were acceptable estimates. Use of the lower limit of 1.4 kcal mol^{-1} for the inherent strain of the hydrogen-bonded conformations set an upper limit for the intrinsic ΔH_i at -3.2 and -3.1 kcal mol^{-1} for **1** and **2**, respectively. Collectively, ΔG_i for the intramolecular hydrogen bonds of **1** and **2** in $CDCl_3$ at 293 K were estimated to be less than -2.1 and -2.4 kcal mol^{-1}, respectively.

Solvent Studies. The H(2)–H(2′) ^3J values for **2** and **10** were also determined (at 20 °C) in a range of solvents to explore the effect of solvation on the rotameric populations and, hence, the free energy of the intramolecular hydrogen bond (*vide infra*). Although ^3J values have been used commonly to evaluate the effect of solvation on conformational equilibria,[10] the solvent dependence of ^3J values intrinsic to a particular conformation have received less attention; generally, solvent-induced changes in ^3J not associated with conformational changes have been small.[28] The ^{1}H NMR analysis of the hydroxyether **2** and the diether **10** also offered an opportunity to evaluate the solvent dependence of intrinsic ^3J values: the H(2)–H(2′) ^3J values report on the solvent-dependent rotameric populations of the hydroxymethyl substituent, while the H(1)–H(6) and H(1)–H(2) ^3J values reflected only the one, heavily biased, chair conformation. In both cases, a similar substituent (hydroxyl or methoxyl) is attached to one of the carbon atoms that defines the dihedral. The observed ^3J values for coupling between H(1) and H(6)β (axial–equatorial) for **2** were 4.22 ± 0.01 Hz in a solvent range of CCl_4 to D_2O, and the average ^3J values for coupling between H(1) and H(6)α/H(2)α (axial–axial) were 10.37 ± 0.07 Hz in all solvents excluding D_2O in which ^3J increased to 10.72 Hz. Clearly, as anticipated, the solvent dependence of the intrinsic ^3J values was small and essentially insignificant relative to observed changes in H(2′) ^3J values (2.4–4.2 Hz) due to changes in rotamer populations.

Graphs of the observed hydroxymethyl H(2)–H(2′) ^3J values for **2** against solvent polarity scales did not demonstrate any significant correlations; for example, a graph of *pro-R* ^3J plotted against the empirical solvent parameter $E_T(30)$ demonstrated considerable scatter (Figure 7a). Graphs of both *pro-R* and *pro-S* ^3J values plotted against other solvent polarity scales such as π^* and solvent dielectric ϵ_K (as the Kirkwood expression:[14] $\epsilon_K = [\epsilon-1][2\epsilon+1]^{-1}$) produced scatter similar to that illustrated in Figure 7a. However, when plotted against the (Kamlet–Taft) empirical solvent hydrogen bond acceptor scale β_{KT}, the ^3J values produced a reasonably linear ($r^2 = 0.935$) relation (Figure 7b);[29] a similar plot of the (Kamlet–Taft) empirical solvent hydrogen bond donor ability α_{KT} (Figure 2a, supplementary material) was not linear. Typically, a minimum of five experimental values per intensive variable would be required for statistically sound pairwise correlations; although **2** was evaluated in nine solvents,[30] approximately linear trends could be "illustrated" with graphs of ^3J plotted against either $E_T(30) + 100\beta_{KT}$ (Figure 7c), $\pi^* + \beta_{KT}$,

(26) Geometries for conformers 2 and 3 for **2** (Figure 3), geometry optimized with AM1, were used to calculate dipole moments at the RHF/3-21G* level giving 1.05 and 2.46 D, respectively. Calculated dipole moments for conformers 1 and 2 of the diether **10** (Figure 3) were 1.00 and 2.24 D, respectively. Conversly, dipole moments calculated for conformers 2 and 4 of the diether **9** (Figure 2), 2.38 and 1.86 D, respectively, were not substantially different, explaining the lack in temperature sensitivity for **9** (and the nonbonded conformers of **1**, *vide infra*).

(27) As noted for **1**, the agreement between calculated ^3J_i values (2.30 and 10.30 Hz) and those predicted[18a,24] from the Karplus relation (2.2 and 10.2 Hz) demonstrates consistency between the IR and ^{1}H NMR analyses.

(28) Laszlo, P. *Prog. Nucl. Magn. Reson. Spectros.* **1967**, *3*, 231. Ando, I.; Asakura, T.; Watanabe, S. *J. Mol. Struct.* **1981**, *76*, 93.

(29) Figures 7a–c demonstrate correlations with the *pro-R* ^3J values only; correlations with the *pro-S* ^3J values were also linear (Figure 2b, supplementary material) but with an opposite slope due to relative magnitudes of the the two ^3J values in the hydrogen-bonded conformation.

(30) The ^{1}H NMR spectra of **2** were also evaluated in a number of other solvents but not included in the data base because $\Delta\delta$ for the AM portion of the spin system (now AB) was small (<10 Hz), which compromised accurate determination of ^3J values.

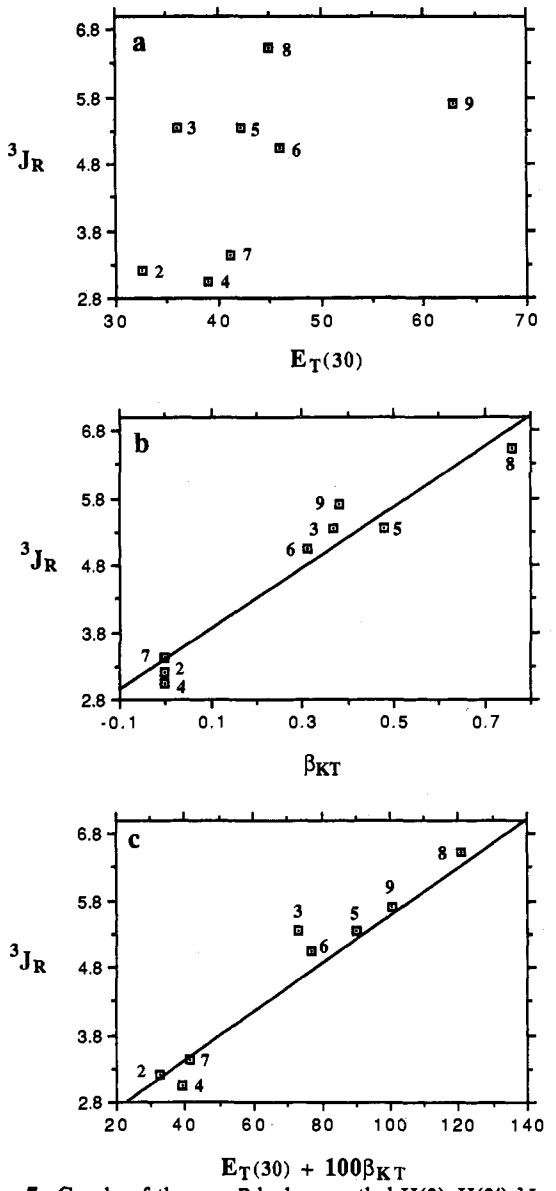

Figure 7. Graphs of the *pro-R* hydroxymethyl H(2)–H(2′) ^3J values (Hz) for **2** plotted against (a) the empirical solvent parameter $E_T(30)$; (b) the (Kamlet–Taft) solvent hydrogen bond basicity β_{KT}; and (c) the sum of $E_T(30) + 100\beta_{KT}$. Solvent numbers: (1) hexane; (2) CCl_4; (3) 1,4-dioxane; (4) $CHCl_3$; (5) acetone; (6) CH_3CN; (7) CH_2Cl_2; (8) DMSO; (9) H_2O. Values were recorded in deuterated solvents.

or $\epsilon_K + \beta_{KT}$ (data not shown). While the linearity with β_{KT} was improved slightly with the sum $E_T(30) + 100\beta_{KT}$ (r^2=0.953), the linearity was slightly decreased when β_{KT} was summed with π^* or ϵ_K (r^2 = 0.833 and 0.873, respectively). However, all of the sums correlated with ^3J within a 95% confidence level (pairwise *t* test) and, thus, must be considered equally valid with respect to the number of solvents evaluated. In the sum with $E_T(30)$, β_{KT} was multiplied by 100 to bring it within the same order of magnitude as $E_T(30)$;[31] otherwise, no attempt was made to optimize the relations. Rather, the approximate linearity seen with simple sums proved adequate to demonstrate the relative importance of both solvent polarity and hydrogen bond acceptor ability as determinants of rotameric populations.[32] A simple test of the validity of these relations was to graph a plot of the methoxymethyl ^3J values for the diether **10**, in which rotameric populations differ only in molecular dipole moments,[26] against solvent polarity scales. The approximately linear relationships

(31) Graphs of ^3J plotted against the sum of β_{KT} and *normalized* $E_T(30)$ values[10] did not produce linear relations.

(32) Sums of solvent polarity scales and α_{KT} gave no linear correlations.

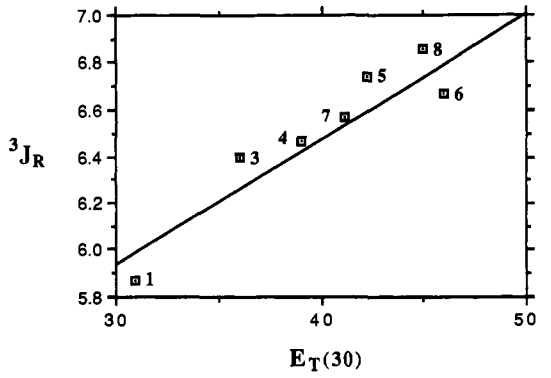

Figure 8. Graph of the *pro-R* methoxymethyl H(2)–H(2′) ^3J values (Hz) for **10** plotted against the empirical solvent parameter $E_T(30)$. Solvent numbers are as in Figure 7.

(r^2 = 0.944–0.887) seen between the diether **10** ^3J values and $E_T(30)$ (Figure 8), π^*, and ϵ_K (Figures 3a,b, supplementary material) demonstrate the anticipated[9-11] dipolar sensitivity to solvent polarity that is overwhelmed by the hydrogen bond solvation in the hydroxyether **2**.

While the H(2)–H(2′) ^3J values for **2** intrinsically reflected relative hydroxymethyl rotameric populations, a more intellectually satisfying relationship between solvent parameters and the intramolecular hydrogen bond ΔG was sought. Thus, intrinsic ^3J values for the hydroxymethyl rotamers of **2** in the hydrogen-bonded and nonbonded states calculated from the temperature data in $CDCl_3$ (see above) were used to convert the ^3J observed in each solvent into a corresponding ΔG. However, a direct conversion using intrinsic ^3J values determined for **2** in $CDCl_3$ at 20 °C into ΔG values produced solvent parameter plots with poor correlations. Rather than a direct conversion, $\langle ^3J_i \rangle$ had to be scaled to the dielectric of each solvent in a manner similar to that done for the calculations of χ^{HB} for **2** at different temperatures in $CDCl_3$. To do so, differences between the observed methoxymethyl ^3J values for the diether **10** in each solvent (Figure 8) and those observed in $CDCl_3$ were applied to $\langle ^3J_i \rangle$, initially calculated in $CDCl_3$, to account for solvent-induced changes in the rotameric populations of nonbonded conformations. The calculated ΔG_{obs} values, averaged from observed *pro-R* and *pro-S* ^3J values, were also corrected for steric strain and ΔS (see above) to give $\langle \Delta G_i \rangle$ values. As observed with ^3J values, graphs of ΔG_i plotted against $E_T(30)$ (Figure 9a), π^*, and ϵ_K (data not shown) were scattered while graphs of $\langle \Delta G_i \rangle$ plotted against β_{KT} (Figure 9b) and the sums $E_T(30) + 100\beta_{KT}$ (Figure 9c), $\pi^* + \beta_{KT}$, and $\epsilon_K + \beta_{KT}$ (Figures 4a,b, supplementary material) produced approximately linear relations (r^2 = 0.808–0.933). The linear relations demonstrate consistency in the use of diether **10** to correct intrinsic ^3J values for the calculation of $\langle \Delta G_i \rangle$ values in each solvent.

Discussion

The hydroxyl–ether hydrogen bond geometries of **1** and **2** should be within the range of experimentally observed geometries to enable a direct application of the observed thermodynamics to other hydrogen bonds. A compilation of hydrogen bond geometries determined from neutron diffraction analyses of sugars[6c] produced mean values for H_d–O_a and O–O atomic distances of 1.82 and 2.77 Å, respectively, and an O–H_d–O_a bond angle of 167°; these were predominantly intermolecular hydrogen bonds which are appropriate for comparisons to, for example, protein intraresidue bonds. Prediction of the hydrogen bond geometries for **1** and **2** was complicated by the inherent compromise between the hydroxymethyl sterics and hydrogen bond energy; thus, the prediction would be only as good as the calculation method. Examination of Table I confirms these expectations: *ab initio* calculations predicted a nearly ideal H_d–O_a bond distance while

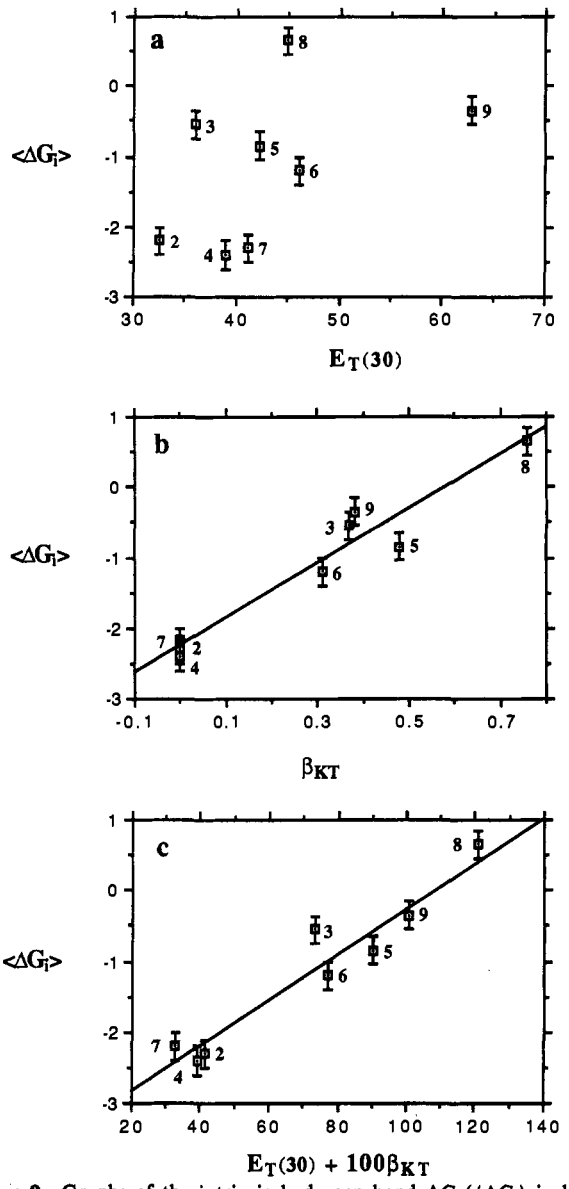

Figure 9. Graphs of the intrinsic hydrogen bond ΔG ($\langle\Delta G_i\rangle$ in kcal mol^{-1}), averaged from the *pro-R* and *pro-S* hydroxymethylene ^3J values for **2**, plotted against (a) the empirical solvent parameter $E_T(30)$; (b) the (Kamlet–Taft) solvent hydrogen bond basicity β_{KT}; and (c) the sum of $E_T(30) + 100\beta_{KT}$. Solvent numbers are asin Figure 7.

both MM2 and AM1 calculations predicted geometries that are 3–4 standard deviations removed from the means observed in neutron diffraction data of carbohydrates.[6c] As a realistic geometry undoubtedly lies somewhere between the two extremes, the intramolecular hydrogen bond in a molecule that has been examined by neutron diffraction,[19] D-α-fructopyranose, was also evaluated to calibrate the calculation methods. Examination of the results (Table II) suggests that all three methods reasonably reproduce experimental geometries; thus, the source of the discrepancy between the calculated geometries for **1** and **2** remains unclear.[33]

The simple correlation of the hydrogen bond free energy with the β_{KT} (Figure 9b) would argue that specific interactions between solvent and the hydrogen bond donor are major determinants of hydrogen bond energetics. Although correlations with β_{KT} summed with solvent polarity scales are also significant, it appeared as if polarity may be a second-order perturbation on the observed energies, particularly in the low polarity solvents. For both $CDCl_3$ and CCl_4, $\beta_{KT} = 0$; thus, it is suggested that hydrogen bond geometry is the major determinant of the energetics in these solvents. Indeed, it has been well-established that ΔH for a specific hydrogen bond is essentially invariant in low-polarity, noncoordinating solvents.[8,15a-d] Thus, the intrinsic ΔH_is calculated for the hydrogen bond in **1** and **2** in $CDCl_3$, −3.2 and −3.1 ± 0.1 kcal mol^{-1}, respectively, would be expected to approach a gas-phase ΔH (−4.7 kcal mol^{-1} for the methanol–diethyl ether adduct[1a]) if the geometries were similar. As simple bimolecular adducts easily optimize the hydrogen bond geometry, it is suggested that the actual geometry for the intramolecular hydrogen bond in **1** and **2** is less than ideal.[35] Further, the observed[1a] ΔH values for simple bimolecular alcohol–ether adducts in CCl_4 (−2.9 to −3.1 kcal mol^{-1}), which should have geometries similar to those of the gas-phase adducts, may be tainted with changes in the ΔH that are not intrinsic to the hydrogen bond itself.

If, upon formation of the hydrogen bond, internal rotations about the hydroxymethylene C–C and hydroxyl C–O bonds in **1** were completely frozen, the changes in gas-phase ΔS would be −5.3 and −4.2 cal mol^{-1} K^{-1}, respectively (total ΔS = −9.5 cal mol^{-1} K^{-1}).[36] Similarly, the total change in the gas-phase internal rotational ΔS for the loss of the three rotors in **2** would be −14.1 cal mol^{-1} K^{-1}. The intrinsic ΔS_i values calculated for **1** and **2** in $CDCl_3$, −3.5 ± 0.5 and −2.4 ± 0.5 cal mol^{-1} K^{-1}, respectively, are less negative than might have been expected, although the ΔS determined[16] for the intramolecular hydrogen bond in 2-methoxyethanol is similar (−4.4 cal mol^{-1} K^{-1}). In addition, it was anticipated that ΔS for **2** would be more negative than for **1**, but the opposite was observed. However, it could be argued that ΔS for **1** and **2** are essentially the same (due to the inherent uncertainty of ΔS values calculated from van't Hoff analyses). In either case, the attenuated losses in ΔS relative to gas-phase calculations may represent greater contributions to the entropy of hydrogen-bonded states from the introduction of low-frequency vibrational modes than had been recognized.[3,37] In **2**, for example, the hydrogen bond may "wag" more than in **1**, which would effectively compensate for the additional hindered rotor involved in the bond. Also, the contribution of internal rotations to the entropy of a molecule in condensed phases may be more complicated than is appreciated; it has been argued that translational and rotational entropies in condensed phases arise from *correlations* between the solute and solvent degrees of freedom,[38] a relationship that is conceptually divergent from that in the gas phase. Clearly, in either case, losses of internal rotational ΔS intrinsic to the formation of a hydrogen bond are not nearly of the magnitude previously assumed.

In studies of solvent effects on the ^{1}H NMR spectra of stabilized enols,[15e-f] it was demonstrated that β_{KT} was the major solvent parameter that correlated with hydroxyl chemical shifts. The correlation was shown to arise from a strong hydroxyl hydrogen bond with coordinating solvents, such as DMSO in CCl_4, and a weak bond with the aromatic face of mesityl substituents in noncoordinating solvents. It remained to be seen whether this correlation would translate to the ΔG of more strongly coordinated hydrogens and ultimately to hydrogen bonds in biological molecules. The analysis of the hydroxyether **2** in a broad range of solvents demonstrated that the ΔG of the intramolecular

(33) While *ab initio* calculations optimally reproduced the D-α-fructopyranose hydrogen-bond geometry it could not be assumed that *ab initio* calculations for **1** and **2** were optimal due to the wide dispersion seen with the different methods for **1** and **2** relative to that seen with the sugar. Also, it has been argued[34] that *ab initio* calculations at MP2/6-31G* levels with basis set superposition errors are required to adequately model hydrogen bonds.

(34) Zahradnik, R.; Hobza, P. *Pure Appl. Chem* **1988**, *60*, 245.

(35) It is noted that the ΔH_i (and ΔG_i) values represent upper limits due to the assumption of less than a 10% population of the bonded conformation in the absence of the hydrogen bond interaction.

(36) Benson, S. W. *Thermochemical Kinetics*, 2nd ed.; John Wiley & Sons: New York, 1976.

(37) (a) Page, M. I.; Jencks, W. P. *Proc. Natl. Acad. Sci. U.S.A.* **1971**, *78*, 1678. (b) Jencks, W. P. *Adv. Enzymol.* **1975**, *43*, 219. (c) Jencks, W. P. *Proc. Natl. Acad. Sci. U.S.A.* **1981**, *78*, 4046.

(38) Lazaridis, T.; Paulaitis, M. E. *J. Phys. Chem.* **1992**, *96*, 3847.

hydroxyl–ether hydrogen bond, as observed from the hydroxymethyl ^1H–^1H NMR ^3J values, does indeed correlate strongly with β_{KT} (Figures 7b and 9b). Such a result has profound implications for hydrogen bonding in biological molecules. Two rather divergent views have evolved regarding the effect of the dielectric within a protein interior on electrostatic interactions: it has been argued that (1) the local dielectric is extremely important to electrostatic energetics or (2) the strongly coordinating environment within a protein renders the concept of dielectric meaningless.[39] The results for the hydroxyl–ether hydrogen bond argue strongly in favor of the latter view; similar results also have been observed with ion pairs.[31] For example, no ΔG_i correlation was observed with any of the solvent polarity scales $E_t(30)$, π^*, and ϵ_K (Figure 9a). These results would also argue that any attempt to account for solvation of hydrogen-bonded molecules with models for solvent polarity alone would be deficient. Rather, the reasonable correlations with sums of solvent polarity scales and β_{KT} (Figures 7c and 9c) would suggest that the most reasonable models for solvation of hydrogen-bonded molecules must include both solvent polarity *and* its propensity to accept a hydrogen bond, with the latter term being strongly dominant. The lack of correlation between the solvent hydrogen bond acidity α_{KT} and hydrogen bond ΔG_i (Figure 3a, supplementary material) was surprising; however, the $E_T(30)$ scale is often considered to be a solvent hydrogen bond acidity scale adjusted to polarity and cohesive density.[8-11] For example, sums of solvent polarity alone (either ϵ_K or π^*) and with β_{KT} produced correlations with slightly diminished linearity relative to β_{KT} alone. Thus, the improved linearity seen between ΔG_i and the sum: $E_T(30) + 100\beta_{KT}$ is due primarily to the solvent hydrogen bond acidity component of $E_T(30)$. Indeed, proposed models for solvation that incorporate solely $E_T(30)$ and hydrogen bond basicity scales, including β_{KT}, have been correlated with many other physicochemical processes.[11]

In the development of solvation models, correlations between empirical solvent polarity scales clearly are inadequate due to the lack of corresponding molecular models. However, the reasonable correlation between ΔG_i and the sum $\epsilon_K + \beta_{KT}$ (Figure 4b, supplementary material) is particularly promising: ϵ_K is the cornerstone of reaction field models[14] for solvation that have already shown great promise in the modeling of solvation effects.[12,13] Also, β_{KT} is related[40] to the solvent molecular electrostatic potential and is, thus, a conceptually satisfying parameter; it remains to be seen if β_{KT} can be incorporated into continuum models of solvation.[12-14] It is also interesting to note that water was well-correlated in each of the relations and is thus not a "unique" solvent, in parallel to previous studies of molecular inclusion phenomena by Diederich and colleagues.[10l,n,o]. Indeed, in any of the summed correlations, DMSO is more "polar" with respect to hydroxyl solvation. Similarily, 1,4-dioxane appears to be more polar than might have been expected (Figures 7c and 9c), which is consistent with the "dioxane anomoly" noted in other studies.[9f,10q,11e] For a linear relation to exist between ΔG_i and a solvent parameter, one of two possibilities is likely: (1) one of the two terms ΔH or ΔS remains constant and the other is proportional to the solvent parameter or (2) both terms may be proportional. While correlations have been demonstrated with hydrogen bond ΔHs in noncoordinating solvents,[8,15] the correlation with β_{KT} reflected specific interactions between the solvent and hydrogen bond donor which would incur changes in both ΔS and ΔH. This further complicates incorporation of the solvent effects into computational models as ΔS is frequently not included in calculation methods.

The observed ΔG_i for the hydroxyl–ether hydrogen bond of **2** in any one solvent is dependent upon the solvation, geometry (undetermined), and any systematic errors[35] in the calculations. Thus, direct application of the ΔG_i to other hydrogen bonds is questionable. However, the *difference* in ΔG_i between two different solvents ($\Delta\Delta G_i$), which reflects only a solvation ΔG, may have more universal applications. Due to the reasonable correlation observed between ΔG_i and the sum $E_T(30) + 100\beta_{KT}$ (Figure 9c, $r^2 = 0.933$) and the widespread use of $E_T(30)$ values in the recent literature, linear regression has been used to derive a relation to predict the change in an observed hydrogen bond free energy between any two solvents:

$$\Delta\Delta G_i = (-3.3 \times 10^{-2})\Delta[E_t(30) + 100\beta_{KT}] \text{ kcal mol}^{-1} \quad (2)$$

Undoubtedly, eq 2 can be applied to other hydroxyl–ether hydrogen bonds and may have broader applications. However, it must be noted that the correlation is not excellent and may require further elaboration. Also, the correlation exists for an *intrinsic* ΔG obtained for an intramolecular hydrogen bond; ΔGs observed for intermolecular hydrogen-bonded adducts undoubtedly experience a solvation ΔG that is unrelated to the hydrogen bond and must be accounted for separately.

Conclusion

Although the hydroxyethers **1** and **2** are not biological in origin and were evaluated in a number of organic solvents, the resulting correlations with solvent parameters have an impact on the general description of similar interactions in biomolecules. Both **1** and **2** structurally mimic individual hydrogen bonds in macromolecular ensembles—since the individual interactions are preorganized for bond formation, losses in bond ΔG resulting from energy expended in molecular reorganizations are minimized. Accordingly, the exquisite sensitivity of the hydrogen bond energetics to solvent hydrogen bond basicity argues strongly in favor of a view in which the strength of a hydrogen bond in the interior of protein is relatively insensitive to local dielectric and may approach that of a gas-phase value if involved with only one acceptor. Further, the relatively minor losses in ΔS due to losses in internal rotations argue that in changes in solvation, translational and rotational entropies may entirely dominate observed ΔS values for receptor–ligand and enzyme–substrate complexes. While these correlations are limited to the observation of hydroxyether hydrogen bonds, they may have more general utility in the description of electrostatic effects. Indeed, ion pair free energies have been correlated to changes in the surrounding polarity environment in proteins[41] and are a function of the particular donor–acceptor capacities of a similar range of solvents that were used in this work.[42] Ultimately, the complementary nature of evaluations of electrostatic interactions and their solvation for inter[1-4] and intramolecular[1j,5] processes are needed to ferret out those principles fundamental to a complete molecular description of electrostatic interactions.

Experimental Section

General Procedures. THF and ether were distilled from benzephenone ketyl; column chromatography was done on silica gel, 230–400 mesh with 10% ethyl acetate in hexanes eluent (unless noted otherwise). Standard workup began with extraction with ether. Combined ether extracts were subsequently dried over $MgSO_4$, decanted, and evaporated on a rotary evaporator. ^1H NMR spectra were recorded with a digital resolution of 0.1 Hz and were resolution-enhanced with a combined Gaussian–exponential function. IR spectra were obtained from $CHCl_3$ solutions in a 1-mm-pathlength cell (NaCl plates).

Ethyl 3-(3-Chloropropyl)-2-hydroxycyclohexanecarboxylate (4). nBuLi (60 mmol) was added dropwise to a stirred solution of diisopropylamine (67 mmol) in 100 mL of THF at 0 °C. After 30 min, the solution was cooled to −78 °C and a solution of ethyl 2-oxocyclohexanecarboxylate (**3**) (30.8 mmol) in 20 mL of THF was added over 5 min. After 30 min, HMPA (32 mmol) and 1-chloro-3-iodopropane (28.8 mmol) were added

(39) The issue of protein dielectric has been discussed: Warshel. A.; Aqvist, J. *Annu. Rev. Biophys. Biophys. Chem.* **1991**, *20*, 267. King, G.; Lee, F. S.; Warshel, A. *J. Chem. Phys.* **1991**, *95*, 4366. See also ref 2j.

(40) Murray, J. S.; Ranganathan, S.; Politzer, P. *J. Org. Chem.* **1991**, *56*, 3734.

(41) Hwang, J. K.; Warshel, A. *Nature (London)* **1988**, *334*, 270.

(42) Beeson, C.; Dix, T. A., manuscript in preparation.

and the solution was warmed to room temperature over 2 h. Workup gave 7.5 g of crude ketoester which was used without further purification. $NaBH_4$ (63 mmol) was added to a stirred solution of the crude ketoester in 100 mL of dry methanol at 0 °C. After 6 h, workup and chromatography gave 1.2 g of **2** (17% yield) as a clear oil: ^1H NMR (500 MHz, $CDCl_3$) δ 4.20 (q, 2 H, J = 7.1 Hz), 4.14 (s, 1 H), 3.58 (td, 2 H, J = 6.5, 1.9 Hz), 2.95 (br s, 1 H), 2.38 (td, 1 H, J = 8.3, 1.4 Hz), 2.0–1.7 (m, 5 H), 1.65 (m, 1 H), 1.45 (m, 5 H), 1.31 (t, 3 H, J = 7.2 Hz); ^{13}C (125 MHz, $CDCl_3$) δ 175.9, 67.8, 60.5, 47.7, 45.1, 40.7, 30.1, 29.9, 25.4, 25.1, 22.8, 14.0; HRMS (CI) exact mass calculated for MH^+ $C_{12}H_{21}O_3ClH^+$ 249.1257, found 249.1261.

10-(Ethoxycarbonyl)-(2-oxabicyclo[4.4.0]decane) (5). NaH (1.4 mmol) was added to a solution of **2** (1.2 mmol) in 60 mL of ether. After 72 h, workup and chromatography gave 180 mg of **3** as a clear oil (71% yield): ^1H NMR (500 MHz, $CDCl_3$) δ 4.23–4.08 (m, 2 H), 3.98 (dd, 1 H, J = 11.6, 4.2 Hz), 3.91 (br s, 1 H), 3.37 (td, 1 H, J = 11.8, 2.0 Hz), 2.36 (td, 1 H, J = 6.8, 2.6 Hz), 1.9–1.65 (m, 6 H), 1.65–1.5 (m, 2 H), 1.32–1.15 (m, 3 H), 1.24 (t, 3 H, J = 7.0 Hz); ^{13}C NMR (125 MHz, $CDCl_3$) δ 173.5, 76.6, 69.2, 60.0, 47.7, 35.4, 29.1, 24.7, 24.4, 21.7, 20.9, 14.1; HRMS (EI) exact mass calculated from M^+ $C_{12}H_{20}O_3$ 212.1412, found 212.1425.

10α-(Hydroxymethyl)-(2-oxabicyclo[4.4.0]decane) (1). A solution of **4** (0.40 mmol) in 10 mL of ether was added dropwise to a stirred solution of $LiAlH_4$ (0.42 mmol) in 20 mL of ether at 0 °C. After 90 min, workup and chromatography gave 40 mg of **1** as a clear oil (59% yield): ^1H NMR (500 MHz, $CDCl_3$) δ 3.99 (dd, 1 H, J = 11.2, 4.7 Hz), 3.78 (dd, 1 H, J = 10.8, 3.2 Hz), 3.70 (br s, 1 H), 3.62 (dd, 1 H, J = 10.9, 5.0 Hz), 3.44 (td, 1 H, J = 11.9, 2.4 Hz), 2.52 (br s, 1 H), 2.0–1.7 (m, 4 H), 1.63 (td, 2 H, J = 12.9, 3.8 Hz), 1.6–1.42 (m, 3 H), 1.4–1.25 (m, 3 H); ^{13}C (125 MHz, C_6D_6) δ 79.2, 69.2, 66.8, 44.4, 36.3, 29.6, 26.3, 25.6, 23.8, 21.8; HRMS (CI) calculated for MH^+ $C_{10}H_{18}O_2H^+$ 171.1385, found 171.1374.

Ethyl 5-*tert*-butyl-2-hydroxycyclohexanecarboxylate (7). $NaBH_4$ (1.1 mmol) was added to a solution of methyl 5-*tert*-butyl-2-oxocyclohexanecarboxylate[17] (**6**) (0.95 mmol) in 50 mL of dry CH_3OH at 0 °C. After 1 h, the reaction was quenched with CH_3CO_2H; standard workup and chromatography gave **7** (31% yield) as a white solid: ^1H NMR (500 MHz, $CDCl_3$) δ 3.73 (s, 3 H), 3.74–3.72 (m, 1 H), 2.73 (br s, 1 H), 2.29 (dt, 1 H, J = 11.02, 3.67 Hz), 2.08–2.04 (m, 2 H), 1.82–1.79 (m, 1 H), 1.31 (dq, 1 H, J = 4.76, 1.74 Hz), 1.16–1.06 (m, 3 H), 0.86 (s, 9 H); ^{13}C NMR (500 MHz, $CDCl_3$) δ 175.84, 71.10, 51.84, 51.30, 46.86, 33.73, 32.38, 29.07, 27.54, 25.16; HRMS (CI) exact mass calculated for MH^+ $C_{12}H_{22}O_3$ 215.1615, found 215.1633.

2-(Hydroxymethyl)-4-*tert*-butylmethoxycyclohexane (2). Excess NaH (60% dispersion in mineral oil) was added to a solution of the hydroxyester **7** (0.90 mmol) and excess CH_3I in 20 mL of ether. After 12 h, standard workup gave the crude methoxyester **8**, which was used without further purification. $LiAlH_4$ was added to a solution of **8** in 50 mL of ether at 0 °C; after 1 h the solution was quenched with NH_4Cl(aq) followed by 10% H_2SO_4. Standard workup and chromatography (20% EtOAc/hexanes) gave **2** as a viscous oil (64% yield from **7**): ^1H NMR (500 MHz, $CDCl_3$) δ 3.63 (dd, 1 H, J = 10.67, 8.20 Hz), 3.53 (dd, 1 H, J = 10.75, 3.20 Hz), 3.37 (s, 3 H), 3.04 (dt 1 H, J = 10.28, 4.14 Hz), 2.90 (br s, 1 H), 2.22 (qd 1 H, J = 12.00, 3.92, 3.85 Hz), 1.81 (td, 1 H, J = 13.07, 3.15 Hz), 1.79–1.08 (m, 3 H), 1.18–1.08 (m, 2 H), 0.96 (dt, 1 H, J = 12.77, 3.34 Hz), 0.841 (s, 9 H), 0.72 (q, 1 H, J = 8.54 Hz); ^{13}C NMR (500 MHz, $CDCl_3$) δ 86.07, 68.92, 55.71, 46.90, 44.94, 32.25, 30.10, 28.64, 27.52, 25.05; HRMS (CI), exact masss calculated for MH^+ $C_{12}H_{24}O_2H^+$ 201.1854, found 201.1842.

10α-((Methoxy)methyl)-(2-oxabicyclo[4.4.0]decane) (9). Excess KH and CH_3I were added to a solution of **1** (90 μmol) in 10 mL of ether. After 8 h, workup and chromatography gave 14 mg of **2** as a clear oil (85% yield): ^1H NMR (300 MHz, $CDCl_3$) δ 4.01 (dd, 1 H, J = 11.6, 4.4 Hz), 3.58 (br s, 1 H), 3.50 (dd, 1 H, J = 9.2, 7.3 Hz), 3.45 (td, 1 H, J = 11.9, 2.3 Hz), 3.39 (s, 3 H), 3.25 (dd, 1 H, J = 9.2, 6.7 Hz), 2.0–1.6 (m, 6 H), 1.6–1.45 (m, 2 H), 1.45–1.2 (m, 4 H); ^{13}C (125 MHz, $CDCl_3$) δ 76.05, 74.92, 69.07, 58.43, 42.32, 35.62, 29.23, 25.48, 25.13, 23.63, 21.47; HRMS calculated for MH^+ $C_{11}H_{20}O_2H^+$ 185.1541, found 185.1523.

1-Methoxy-2-((methoxy)methyl)-4-*tert*-butylcyclohexane (10). Excess NaH (60% dispersion in mineral oil) was added to a solution of **2** (0.48 mmol) and excess CH_3I in 25 mL of ether. After 48 h, workup and chromatography gave the diether **10** (88% yield) as a clear oil: ^1H NMR (500 MHz, $CDCl_3$) δ 3.49 (dd, 1 H, J = 9.03, 2.92 Hz), 3.39 (dd, 1 H, J = 9.00, 6.43 Hz), 3.34 (s, 3 H), 2.89 (dt, 1 H, J = 10.58, 4.39 Hz), 2.19 (qd, 1 H, J = 12.79, 3.09 Hz), 1.79 (td, 1 H, J = 12.41, 2.98 Hz), 1.152–0.905 (m, 8 H). 0.848 (s, 9 H); ^{13}C NMR (500 MHz, $CDCl_3$) δ 80.19, 74.46, 59.02, 56.36, 47.13, 44.15, 32.38, 30.81, 29.84, 27.65, 25.46; HRMS (CI) exact mass calculated for MH^+ $C_{13}H_{26}O_2H^+$ 215.2001, found 215.2000.

Acknowledgment. We thank the donors of the Petroleum Research Fund, administered by the ACS (Grant 21426-G4), and the University of California Cancer Coordination Research Committee for financial support of this research (to T.A.D.). C.B. is grateful for support as a National Institutes of Health predoctoral trainee (GM07311). The computer hardware was purchased with instrument funds from the National Institutes of Health (RR-05690) to T.A.D.

Supplementary Material Available: ^1H NMR spectra for new compounds and Figures 1–4 described in the text (11 pages). Ordering information is given on any current masthead page.